JOURNAL OF MATERIALS SCIENCE 33 (1998) 3017–3029

The effect of composition on the microwave bonding of alumina ceramics

J. G. P. BINNER*, J. A. FERNIE[§,‖], P. A. WHITAKER*[,¶], T. E. CROSS[‡]
*Departments of Materials Engineering and Materials Design and [‡]Electrical and Electronic Engineering, The University of Nottingham, University Park, Nottingham, UK
[§] TWI, Abington Hall, Abington, Cambridge, UK
E-mail: jon.binner@nottingham.ac.uk.

The microwave bonding of three alumina ceramics with different compositions has been investigated, without the use of interlayers, using a single-mode resonant cavity operating at 2450 MHz. The temperature and axial pressure were varied and the bonding time was kept to a minimum. For comparison, equivalent joins were produced using a standard diffusion bonding technique. Analysis of the resultant bonds indicated that, the lower the purity of the alumina, the more successful is the microwave bonding process. Whilst 99.8% alumina could not be heated to sufficiently high temperatures, the 94% and 85% aluminas could be joined successfully. The results indicated that a major function of the glassy grain-boundary phase was to increase the dielectric loss of the material. For the 85% alumina, bonding times were typically 10 min or less and total processing times were 30–45 min. This was much faster than could be satisfactorily achieved using diffusion bonding and resulted in significantly less deformation of the samples. The operational mechanisms, however, appeared to be almost identical between the two techniques and were based on viscous flow of the glassy grain-boundary phase. Provided that sufficient migration across the bond line of both glassy phase and grains occurred, then a fully homogeneous microstructure was obtained. In such cases, the mechanical strength of the bond could be at least as high as and often higher than that of the parent material, with the joined samples never breaking at the bond line during four-point bend tests.

1. Introduction

The exploitation of ceramics in an expanding field of engineering applications has resulted in the need for changes in both component design and fabrication. However, the high hardness and lack of ductility in ceramics have resulted in limitations on the complexity of shapes which can be formed without extensive machining and hence high costs. One alternative is the fabrication of smaller, simpler shapes which can be moulded with better quality and then joined together to form the final component. This approach places the emphasis on the need to establish bonding techniques which are simple, fast and inexpensive and yet yield bonds that will deliver the performance required of the ceramic component.

The ability to form rapid high-quality bonds between a range of ceramic materials using microwave energy has been demonstrated by a number of researchers using two main approaches, namely, direct and indirect joining. In the latter case, use is made of some form of interfacial layer to assist in achieving bonding. Engineering ceramics which have been investigated to date include Al_2O_3 [1–10], mullite [3], Si_3N_4 [1–3, 10] and SiC [11–15]. Rods, tubes and bars of various sizes have all been joined.

Fukushima *et al.* [1, 2] investigated the microwave bonding of different grades of alumina. They found that relatively low-purity (96% or less) materials could be joined readily whilst high-purity (99% or greater) ceramics were insufficiently lossy to heat, making direct joining difficult. Characterization of the joined samples showed only minor differences before and after bonding. Although no grain growth or cracking was evident, the local hardness was found to increase in the bond region. Similar results were found by Palaith *et al.* [3] when working with alumina and in all cases evidence was found that the grain-boundary phases had been melted during the process. The strengths of the bonded materials were at least as strong as and often stronger than the base material [1–3]. The inability to achieve direct bonding in high-purity alumina led to experiments involving lower-purity [1, 2] interlayers. Using this approach, successful bonds were achieved with strengths approaching 90% of the base material. Sealing glasses have also been tried and found to be successful [3–5] as have

[¶] Present address: Morgan Matroc Ltd, St. Peter's Road, Rugby, Warwickshire, CV21 3QR, UK.
[‖] Present address: Morganite Thermal Ceramics Ltd, Liverpool Road, Neston, South Wirral, L64 3RE, UK.

alumina gels [6–8]. The latter have the advantage that, at the bonding temperature, the gel transforms into colloidal α-alumina which subsequently sinters, providing consistency across the bond region. The use of alumina powder intermediaries [9] was less successful in that, although high strengths were achieved, results were more erratic owing to shrinkage cracks caused during sintering within the intermediary. Attempts simultaneously to sinter and join green ceramics with a slip interlayer were more successful [10].

The aims of this work were (i) to investigate the effect of composition on the ability to bond alumina ceramics, without the use of interfaces, using microwave energy and hence (ii) to clarify the microwave heating and ceramic bonding mechanisms.

2. Experimental procedure

2.1. Microwave heating system

A simplified control diagram of the heating system used to carry out the joining experiments is illustrated in Fig. 1. The controllable power source used in the initial work was a 300 W ±2% magnetron operating at 2450 MHz with a peak tolerance of ±10 MHz. However, work on the highest-purity (99.8%) alumina indicated that higher power levels were required so the power source was upgraded to a 1 kW ±5% magnetron. The microwaves were conducted by an electromagnetic transmission line to a resonant applicator in which the ceramic to be joined was held. Incorporated along this transmission line was a 3 kW ferrite three-port isolator with an operating frequency of 2425–2475 MHz. This protected the magnetron against any reflections which could arise owing to mismatches of power coupling between the source and reasonant cavity. The reflected power was monitored using a diode detector. A four-stub tuner was also placed in the transmission line to allow coupling of the microwave source to the resonant applicator to be optimized. The applicator used was a single-mode rectangular cavity which resonated in the TE_{102} mode. This allowed the energy to be "concentrated" at the bond line. The design of the applicator is shown in Fig. 2. It consisted of a straight section rectangular brass waveguide (WG9A) with flange connections to an iris and the four-stub tuner one side and a manually adjusted non-contacting short-circuit double plunger on the other. The iris was a sheet of aluminium 2 mm thick which fitted between the flange connections of the four-stub tuner and applicator. The dimensions of the iris aperture determine the amount of power which can enter the cavity from the magnetron. Although an adjustable iris design was investigated, it was found that a fixed aperture of 25 mm by 35 mm could be used successfully. To assist in monitoring the size of the *E* field within the applicator, a magnetic loop coupler was inserted through a port in the broad wall of the cavity to interact with the *H* field (the *E* and *H* fields being proportional to one another).

Three grades of alumina rods (Coors Ceramics Co, USA) were investigated; details of their compositions and physical characteristics are listed in Table I. The majority of the additives for the 85% and 94% pure ceramics existed in the form of a glassy phase which surrounded the α-Al_2O_3 grains. Rods 10 mm in

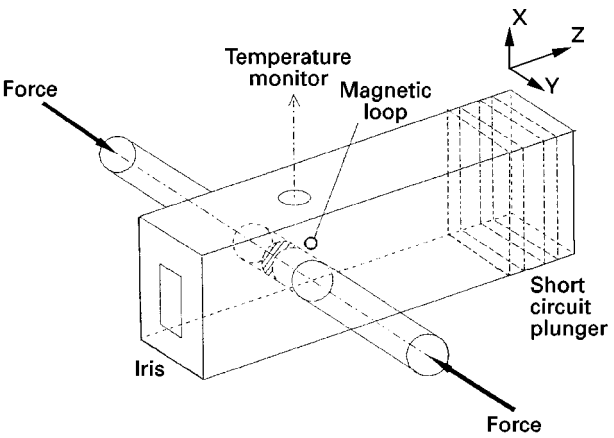

Figure 2 Schematic diagram of the single-mode TE_{102} resonant applicator.

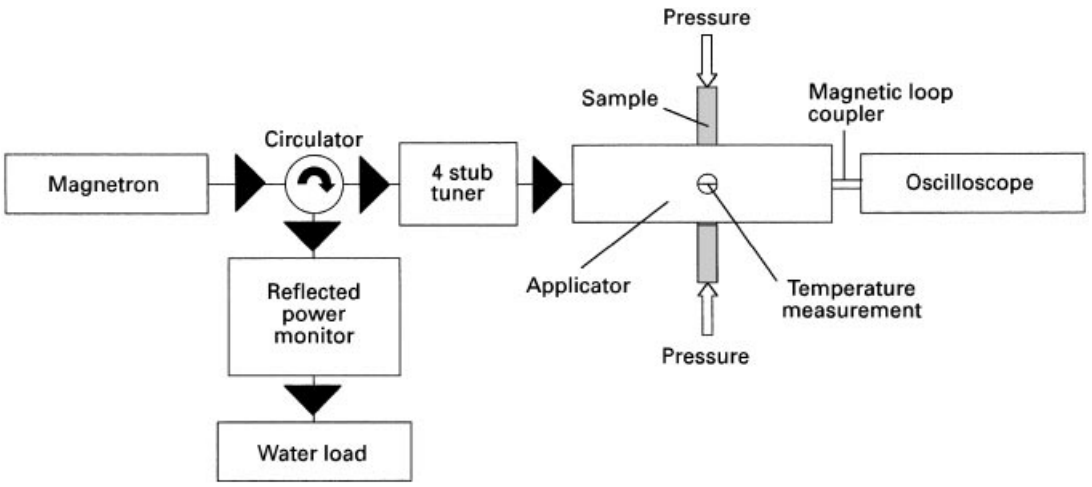

Figure 1 A simplified control diagram for the microwave heating system.

diameter of the three grades of alumina were sectioned into 50 mm lengths and the butting faces diamond ground. The rods were inserted through chokes in the broad wall of the cavity and aligned so that the bonding faces were located at the point of maximum electric field (at $\lambda_g/4$ from the iris, where λ_g is the waveguide wavelength). This ensured that the bond region would be the hot zone during microwave heating. The rods were supported within the cavity by the use of fused quartz tubing and brass plugs, the latter being machined for a close tolerance fit into the choke openings to prevent microwave leakage from the partially filled chokes. The support mechanism is illustrated schematically in Fig. 3. To reduce heat losses the rods were encased in high-purity alumina fibreboard (Fibrefrax Duraboard 1600) from which the polymer binder had been burnt out prior to use. This permitted uniform heating of the bond region; without the insulation, hot spots often developed in the ceramic, leading to thermal runaway. A stainless steel support rig was constructed around the applicator to allow a compressive axial load to be applied to the ends of the rods during the joining cycle (see Fig. 3). The load was maintained at a constant level throughout the heating cycle by releasing the excess pressure resulting from thermal expansion. The surface temperature of the sample was monitored using a lightpipe system (Accufiber Inc., Beaverton, OR, USA) connected via a microprocessor to a personal computer. The sapphire lightpipe was inserted through a choke in the narrow wall of the cavity and clamped into position 1 mm above the butting faces. The manufacturers quote an accuracy of $\pm 5\,^{\circ}C$ for the system as used.

TABLE I Composition and physical characteristics of the three grades of alumina rods (diameter, 10 mm; length, 50 mm) as stated by the manufacturer Coors Ceramic Co, USA

Grade	α-Al_2O_3 (%)	Density ($g\,cm^{-3}$)	Average grain size (μm)
AD85	85	3.41	6
AD94	94	3.70	12
AD99.8	99.8	3.96	3

2.2. Bonding

2.2.1. Microwave bonding

A matrix of microwave bonding experiments was performed for each alumina grade in which the bonding temperature and axial pressure were varied over the ranges 1400–1600 °C and 0.25–1.0 MPa. Heating rates of approximately $3\,^{\circ}C\,s^{-1}$ were used up to about 1200 °C after which the heating rate was reduced (Table II). The time at temperature was kept constant at 10 min and the bonding temperature specified was maintained to $\pm 5\,^{\circ}C$. In all instances the system was initially tuned at low power levels of 10–50 W before increasing to a higher power level (usually 250 W) to commence the heating cycle. Resonant tuning of the applicator was achieved by adjusting the cavity length, d_c, using the plunger to create a standing wave (achieved when $d_c = \lambda_g$) and positioning the four stubs to maximize the impedance matching of the cavity to the external circuit. The reflected power was maintained at a minimum by continuously retuning to compensate for the effect of a change in temperature on the dielectric properties of the sample and subsequent variation in the microwave field distribution. It was noted that once a temperature of approximately 1300–1400 °C was reached, the pressure felt by the sample began to decrease as deformation occurred. Since attempts to maintain the applied axial pressure throughout the entire bonding cycle resulted in buckling of the rods, the applied pressure was allowed to fall to zero once the bonding temperature was reached. At the end of the bonding cycle the power was reduced to zero and the samples were allowed to cool naturally to room temperature. The temperature of the bond region of each pair of samples was continuously monitored using the lightpipe system from the beginning to the end of the heating–cooling cycle.

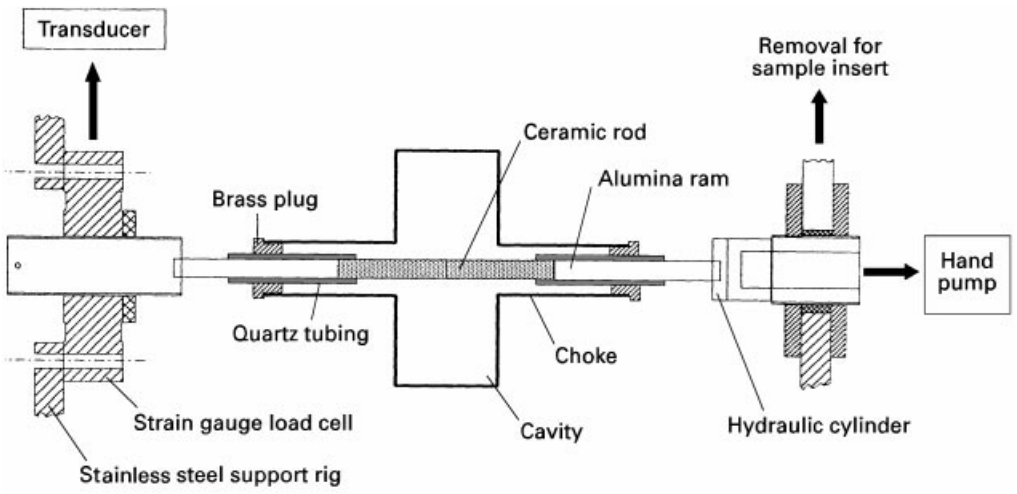

Figure 3 Schematic diagram of the sample support and loading system.

TABLE II Microwave joining conditions for alumina

Property (units)	Value for the following combinations			
	AD85–AD85	AD94–AD94	AD99.8–AD99.8	AD85–AD99.8
Joining or maximum temperature (°C)	1400–1600	1500–1600	1400	1500–1600
Maximum power used (W)	250	250	250	250
Axial pressure (MPa)	0.25–1	0.5–1	1	0.5–1
Typical heating rate ($^{\circ}C\,s^{-1}$)	3.0 at $< 1200\,^{\circ}C$; 0.4 at $> 1200\,^{\circ}C$	2.5 at $< 1000\,^{\circ}C$; 1.0 at $> 1000\,^{\circ}C$	3.0	3.6 at $< 1200\,^{\circ}C$; 0.5 at $> 1200\,^{\circ}C$
Typical cooling rate ($^{\circ}C\,s^{-1}$)	3.0	3.7	4.0	3.5
Holding time (min)	10	10	—	10
Typical total processing time (min)	30	40	25	30

2.2.2. Diffusion bonding

Samples were joined using a conventional diffusion bonding technique under similar processing conditions of temperature, axial load and time in order to allow a comparison of the quality of the bonds produced with that obtained using the microwave heating process. The samples were prepared as described above and then joined using a 450 kHz, 6 kW induction furnace. The samples were enclosed in graphite tooling within the induction coil and the furnace reduced to a 10^{-2}–10^{-3} Pa vacuum to prevent oxidation of the tooling during the heating cycle. A type-R thermocouple was used to measure the bonding temperature and manually controlled heating rates of 0.2–0.7 $^{\circ}C\,s^{-1}$ were used to raise the samples to the bonding temperatures investigated. Holding periods of 0, 15 or 60 min were used after which the power was switched off and the samples allowed to cool to room temperature at rates of 0.1–3.7 $^{\circ}C\,s^{-1}$.

2.3. Characterization

2.3.1. Scanning electron microscopy observation

After joining, the bond region of the rods was sectioned lengthwise, mounted in acrylic resin and polished using normal preparation procedures. Sections from the untreated materials were also prepared in the same manner for comparative studies. After either carbon or gold coating, a scanning electron microscope fitted with an energy-dispersive X-ray detector was used to obtain secondary-electron (SE), back-scattered electron (BSE) and elemental images. When very successful bonds were produced, the only method of determining the location of the bond was via a fortuitous, approximately 100 μm misalignment of the rods which showed up as steps at either end of the bond line. It was then possible to track across the bond line with the scanning electron microscope. A number of the samples were etched in 5% hydrofluoric acid for 10 min to remove the glassy grain-boundary phase and to highlight the grain boundaries.

2.3.2. Deformation effects

The dimensions of each sample were measured both before and after bonding to allow the extent of deformation caused by the thermomechanical cycle to be determined. The measurements were then converted into percentages of the area and longitudinal strain.

2.3.3. Microhardness measurements

Vickers microindentations were performed on the samples using a 3 N load along a series of lines running perpendicular to the bond and spanning a distance of 3 mm either side of the bond. This permitted the relative hardness of the microstructure to be determined since Fukushima *et al.* [1] had found an increase in local hardness at the bond line. Eight randomly distributed indentations were also measured across the section of each untreated alumina grade.

2.3.4. Flexural strength

The flexural strength of the bonds made between the AD85 and AD94 materials when using 1600 °C and 1 MPa as the bonding conditions were measured using four-point modulus-of-rupture tests. Six samples of each grade were measured, together with six samples of each untreated material. Prior to testing, the rods of 10 mm diameter were diamond ground into bars of 7 mm by 7 mm square section to prevent the misalignment of the rods mentioned earlier from having a deleterious effect.

2.3.5. Dielectric properties

The dielectric properties of all three grades of alumina were measured over the frequency range 200–4000 MHz as a function of temperature using a surface probe technique. This has been described in detail elsewhere [16]. To use this technique successfully, each sample needed to be diamond ground to a surface finish of better than 0.5 μm (R_a) surface roughness.

Measurements were made over the temperature range from room temperature to 1200 °C, with individual measurements taken at 40 °C intervals up to 500 °C and at 20 °C intervals thereafter. For each grade, six samples were measured to provide an average value. The estimated error associated with the technique for calculating complex permittivities has been quoted as ± 8% [16].

Using the dielectric property data obtained for all three purities of alumina at 2450 MHz, approximate values were calculated for the glassy grain-boundary phase present in the lower purity AD85 and AD94 ceramics using the refractive index mixture equation [17]

$$\varepsilon_m^{1/2} = v_1\varepsilon_1^{1/2} + v_2\varepsilon_2^{1/2} \quad (1)$$

where ε_m is the permittivity of a mixture comprising two phases of permittivity ε_1 and ε_2 and volume fraction v_1 and v_2 respectively. Values for both AD85 and AD94 were substituted for ε_m and for AD99.8 for ε_2 in separate calculations, and average values for ε_1, the glassy phase, calculated over the temperature range 100–1200 °C. The calculations thus assume that AD99.8 is representative of the composition of the polycrystalline phase in the two lower-purity ceramics.

The alternating-current (a.c.) conductivity, σ, was also calculated from the dielectric loss data ε'' using the equation

$$\sigma = 2\pi_f\varepsilon_0\varepsilon'' \quad (2)$$

where f is the frequency in (hertz) and ε_0 is the permittivity of free space (equal to 8.854×10^{-12} F m^{-1}). Plotting the conductivity data on a natural logarithmic scale against inverse temperature produced an Arrhenius curve which allowed the experimental activation energy for conductivity to be estimated for temperatures above 500 °C.

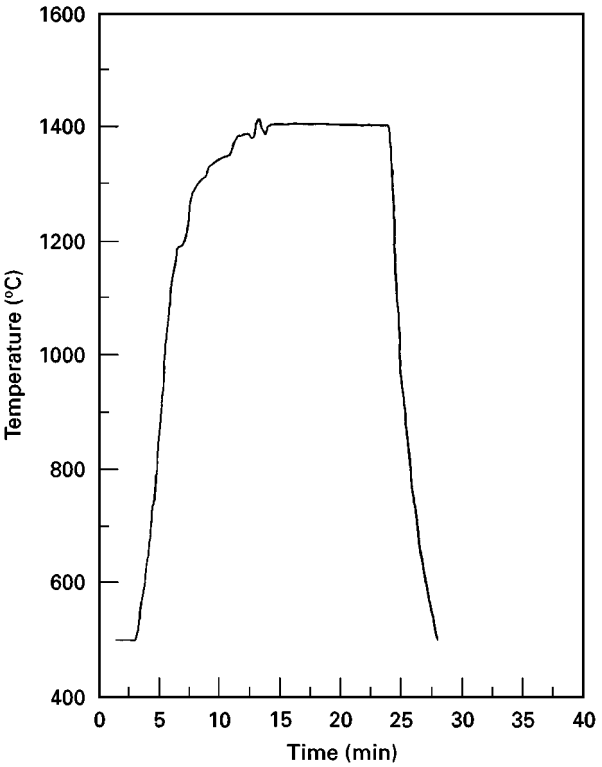

Figure 4 Typical example of a temperature profile for an AD85–AD85 sample, joined at 1400 °C, 0.25 MPa and 10 min holding time.

3. Results

3.1. Microwave bonding

The general processing parameters used are outlined in Table II; specific processing characteristics for each material combination are outlined below. An example of a typical temperature profile as a function of time is shown in Fig. 4.

For *AD85–AD85*, to avoid the development of hot spots and thermal runaway in the material, it was always found essential to reduce the power level below 250 W once the temperature exceeded 1000 °C.

For *AD94–AD94*, in all cases tuning was lost on reaching temperatures in the region of 800–1000 °C. Adjusting the tuning and fluctuating the power level allowed control of the heating cycle to be regained and thermal run-away to be avoided.

For *AD99.8–AD99.8*, owing to the narrow *E*-field peak developed with this grade, the cavity was found to be very sensitive to adjustments to either the end wall or four-stub tuner, and tuning was easily lost during heating. Reducing the size of the iris did not improve the coupling of the system and although the move to a 1 kW magnetron mentioned earlier allowed a higher maximum temperature to be reached (1200–1400 °C versus 1000 °C for the 300 W magnetron), the development of hot spots and thermal runaway were a regular feature.

For *AD85–AD99.8*, the AD85 material was found to couple preferentially with the microwaves resulting in greater deformation of this ceramic under the applied axial pressure. Careful adjustments to the tuning were required to allow bonding temperatures of 1500 and 1600 °C to be reached.

3.1.1. Scanning electron microscopy observation

A summary of the scanning electron microscopy observations made on the microwave bonds is given in Table III; attempts to join the AD99.8 to itself were unsuccessful owing to an inability to heat the material to a sufficiently high temperature. The maximum reached was only 1395 °C. Both AD85 and AD94 could be microwave bonded successfully, however, as could AD85 to AD99.8.

The AD85–AD85 combination joined using the conditions of 1400 °C and 0.25 MPa and shown in Fig. 5 typifies the standard of bond defined as no or negligible contact. The bond line was clearly visible across the width of the sample and regions of contact between the opposing faces were sparsely distributed. As the pressure and/or temperature increased, the quality of the bond improved. By 1500 °C and 0.25 MPa the samples were joined but there were regions of poor contact present in the form of elongated porosity. An increase in axial pressure to 0.5 MPa reduced the extent of the porosity to the outer edges of the sample; the location of the bond

TABLE III Degrees of success achieved in microwave joining alumina rods, where all joins were made using a time of 10 min at joining temperature ((□), no or negligible join; (○), joined but regions of poor contact; (●), successful join)

Temperature (°C)	Degree of success in microwave joining for the following material combinations and pressures						
	AD85–AD85			AD94–AD94		AD85–AD 99.8	
	0.25 MPa	0.50 MPa	1.00 MPa	0.50 MPa	1.00 MPa	0.50 MPa	1.00 MPa
1400	□	○	●				
1500	○	○	●	□	○	○	●
1600	●	●	●	○	●	●	●

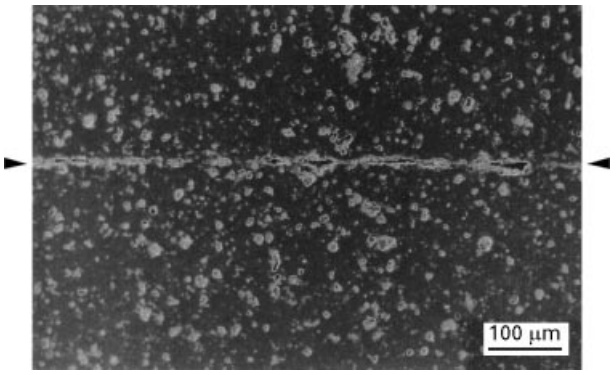

Figure 5 Join made using inadequate conditions (AD85; 1400 °C and 0.25 MPa). The join was clearly visible across the sample.

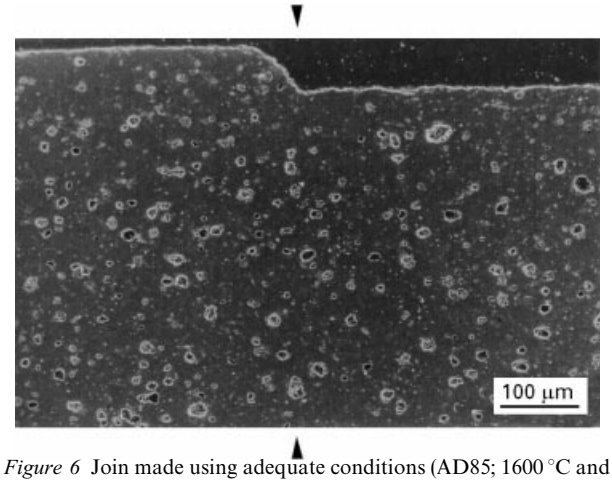

Figure 6 Join made using adequate conditions (AD85; 1600 °C and 0.25 MPa). The join cannot be seen.

disappeared on moving 500 μm into the sample. Increasing the temperature still further to 1600 °C meant that the bond could not be distinguished, except for the slight misalignment of the sample at the edges mentioned earlier, at all pressures examined. Fig. 6 shows the edge of a sample bonded at 1600 °C and 0.25 MPa; note that the microstructure appears completely homogeneous.

Etching of the samples removed the glassy grain-boundary phase so that the position of the grains in the bond region was clearly visible. At 1400 °C, when using a low axial pressure of 0.25 MPa, contact was only made between the peak asperities of the butting faces. Elsewhere a gap of up to 10 μm separated the faces. Increasing the pressure improved the contact between grains from the opposite faces and, at 1 MPa, caused the grains to slide over one another and lock into position. Increasing the temperature to 1500 °C reduced the pressure required to 0.25 MPa in order to attain good contact at the bond across the centre of the sample, as shown in Fig. 7. However, at the edges of the sample a 3–5 μm gap still existed. For the sample joined at 1500 °C and 0.5 MPa the bond line was not visible across the entire specimen (Fig. 8). At 1600 °C, an axial pressure of 0.25 MPa was sufficient to allow continuous contact and to cause the grains from opposing faces to slide over one another (Fig. 7). This figure also shows that at locations where the α-Al_2O_3 grains have come into contact from the two butting faces they appear to have sintered together by atomic diffusion across the interface. The ability to achieve complete continuity across the bond line has been confirmed by elemental distribution maps for aluminium and silicon, shown in Fig. 9 for an AD85 sample joined at 1500 °C and 1 MPa.

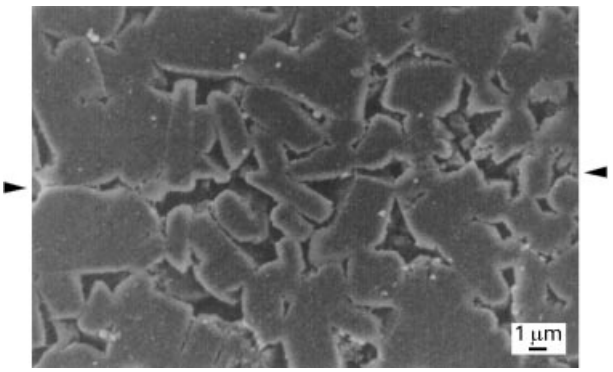

Figure 7 An AD85–AD85 sample joined at 1500 °C and 0.25 MPa in 10 min which has been etched to remove the glass phase and so to outline the positions of the grains at the join.

The AD94–AD94 combinations showed a similar pattern of behaviour to the AD85 material, except that the conditions required for successful bonds were more demanding and, in general, contact between the butting faces decreased towards the centre of the sample. For the AD85 combinations, contact was generally better at the centre of the sample. To achieve an undetectable bond line, conditions of 1600 °C and 1 MPa were required; the bond location could only be ascertained by the slight misalignment of the sample at the edges. Examination of the sample using BSE imaging showed a completely homogeneous microstructure (Fig. 10), the grains having come into contact from the opposing surfaces and rearranged across the bond line. At the lower conditions of either

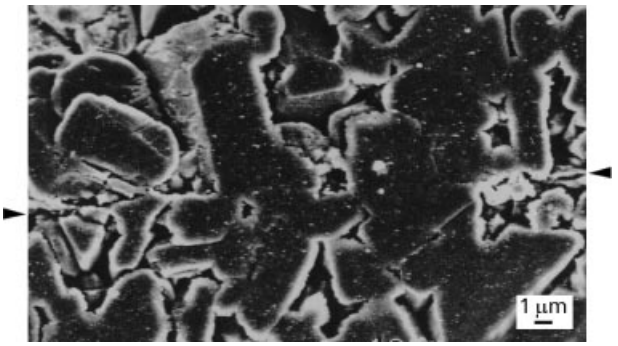

Figure 8 Etched bond line in AD85 at 1500 °C and 0.5 MPa. Evidence can be seen of atomic diffusion joining individual grains and of movement of grains across the bond line.

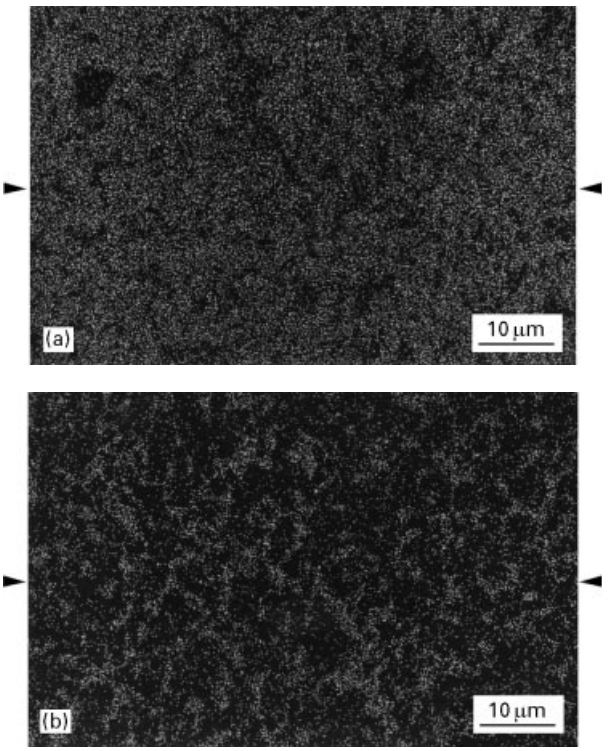

Figure 9 Elemental distribution maps for AD85–AD85 rods joined at 1500 °C and 1 MPa in 10 min: (a) aluminium; (b) silicon. The concentrations of each are continuous across the join.

1600 °C and 0.5 MPa or 1500 °C and 1 MPa, examination using BSE imaging indicated that a clear line of glass phase existed at the join, as shown by the lighter regions in Fig. 11.

For both the AD85–AD85 and the AD94–AD94 material combination, the grain dye did not appear to be affected by the microwave heating process.

For the AD85–AD99.8 combination, examination of the BSE image of joins made using either 1500 °C and 1 MPa or 1600 °C and 0.5 MPa showed a high concentration of glass phase at the bond line, although there were regions where good contact was made between the grains from opposing faces (Fig. 12). At high magnifications, line profiles for the major constituent elements, Al and Si, resulted in a sharp transition being observed (Fig. 13). A few isolated regions of elongated porosity were found across the width of the sample, the largest being about 100 μm long and 10–20 μm wide. Elsewhere the SE image

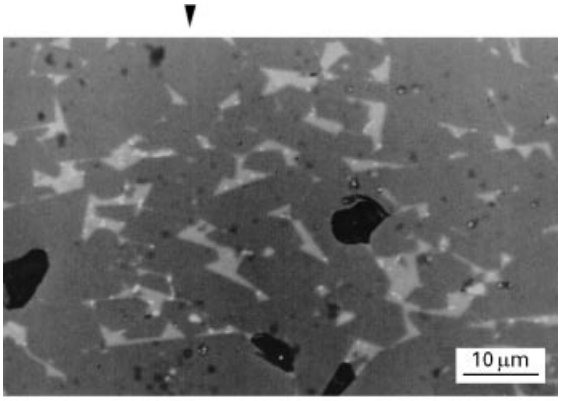

Figure 10 BSE image of join made with AD94 at 1600 °C and 1 MPa. No glass layer can be seen at the bond line.

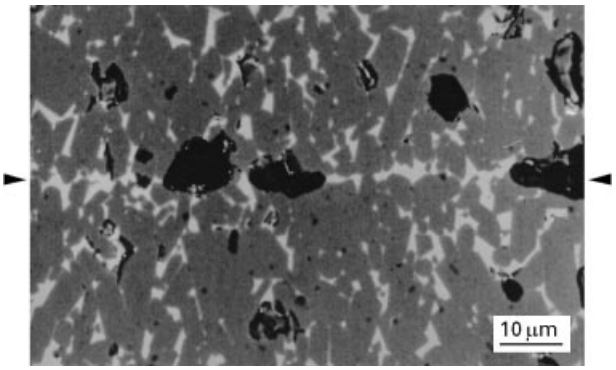

Figure 11 BSE image of an AD94–AD94 sample joined at 1500 °C and 1 MPa in 10 min.

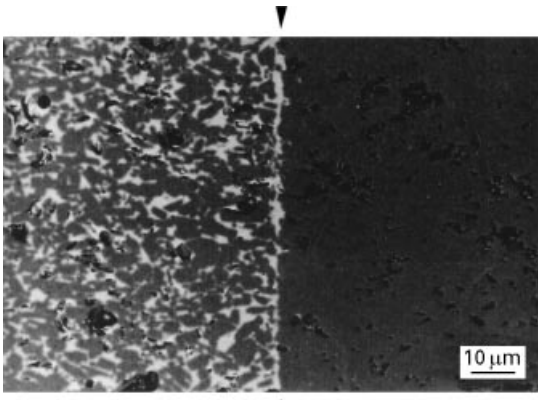

Figure 12 BSE image of join made between AD85 and AD99.8 at 1600 °C and 0.5 MPa. A glass layer can be seen at the bond line.

indicated complete continuity across the join. When the conditions were raised to 1600 °C and 1 MPa, the bond line became completely undetectable using SE imaging. The BSE image indicated that a clear line of glass phase 5–10 μm thick existed at the bond, although there were regions where the grains appeared to project through from the AD85 material and to make contact with the AD99.8 surface.

3.1.2. Deformation effects

The effective hot zone created during the heating cycle spanned a length of approximately ± 5 mm centred at

the bond line. Within this hot region a general increase in sample diameter was observed with the extent of the deformation governed by the bonding temperature and applied axial pressure. A consequent reduction in sample length was also observed. The percentage area strain, ε_a, across the bond region, and longitudinal strain, ε_l, were measured for most samples and the results are summarized in Table IV. It may be observed that both forms of deformation increased with increasing temperature and applied axial force as expected. In a number of samples, particularly for the AD85–AD85 combination, uneven deformation across the bond area occurred, leading to an exaggerated area strain on the side of the sample closest to the iris. This resulted from the slight movement of the hot zone away from the bond line due to the effective change in the waveguide wavelength, λ_g, as a result of the changing dielectric properties of the sample on heating. In Table IV, this effect has been averaged out for the area strain calculations. Excess bulging of the AD85–AD99.8 combination about 10 mm away from the join in the AD85 material was also observed. SEM examination of the material in this region suggested that the glass phase in the lower-purity alumina had significantly softened and the size and amount of porosity had increased. This is believed to have occurred as a result of the differing dielectric properties of the two grades of alumina which resulted in the lower-purity grade heating preferentially.

3.1.3. Microhardness measurement

Fig. 14 shows the hardness distribution for 3 mm on each side of the bond line of a good-quality

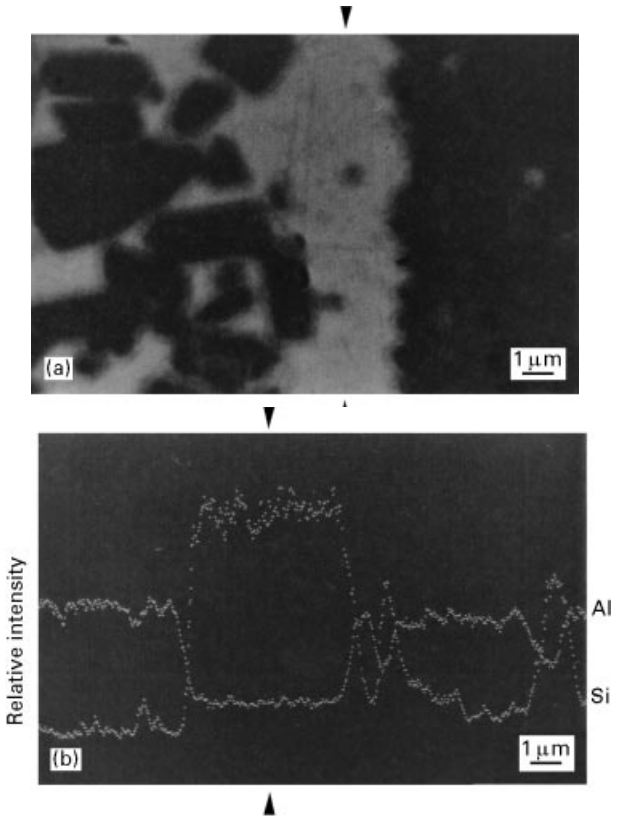

Figure 13 (a) BSE image of an AD85–AD99.8 sample joined at 1500 °C and 1 MPa in 10 min; (b) the corresponding elemental line maps for Al and Si.

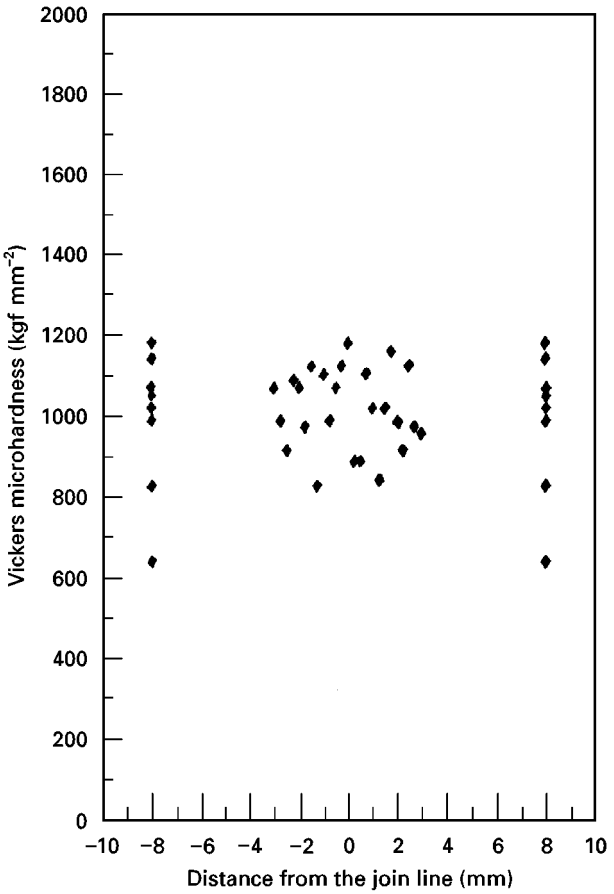

Figure 14 Vickers microhardness measurements across the bond line for an AD85–AD85 sample joined at 1600 °C and 1 MPa in 10 min.

TABLE IV Measured areas and longitudinal strains for the microwave joined alumina samples

Temperature (°C)	Measured area and longitudinal strain for the following material combinations and pressures						
	AD85–AD85			AD94–AD94		AD85–AD99.8	
	0.25 MPa	0.50 MPa	1.00 MPa	0.50 MPa	1.00 MPa	0.50 MPa	1.00 MPa
1400	$\varepsilon_a = +2.9$, $\varepsilon_l = -0.3$	—	$\varepsilon_a = +5.6$, $\varepsilon_l = -0.3$	—	—	—	—
1500	—	—	$\varepsilon_a = +6.2$, $\varepsilon_l = -0.5$	$\varepsilon_a = +0.4$, $\varepsilon_l = -0.1$	$\varepsilon_a = +1.0$, $\varepsilon_l = -0.2$	$\varepsilon_a = +4.3$, $\varepsilon_l = -0.3$	$\varepsilon_a = +4.7$, $\varepsilon_l = -0.4$
1600	$\varepsilon_a = +6.8$, $\varepsilon_l = -0.4$	—	$\varepsilon_a = +8.3$, $\varepsilon_l = -0.5$	$\varepsilon_a = +1.5$, $\varepsilon_l = -0.3$	$\varepsilon_a = +4.7$, $\varepsilon_l = -0.4$	$\varepsilon_a = +5.9$, $\varepsilon_l = -0.3$	$\varepsilon_a = +7.9$, $\varepsilon_l = -0.5$

AD85–AD85 join (1600 °C and 1 MPa). A wide scatter of values was observed; however, all remained within the range of the untreated bulk material. The latter are shown at $\pm$ 8 mm for comparison. A similar result was obtained for the AD94–AD94 sample joined under the same processing conditions although the mean hardness was slightly higher at 10.81 $\pm$ 3.15 GPa (cf. 9.88 $\pm$ 2.02 GPa for the AD85 combination).

3.1.4. Flexural strength

The maximum stress to fracture σ_{max}, during four-point bend testing, was calculated from the measured peak loads at failure for both the untreated and the microwave joined samples of AD85 and AD94. The average σ_{max} values for each case are given in Table V. Examination revealed that all the AD85 samples fractured remote from the bond, the cracks initiating from random locations on the tensile surface within the loading span. All of the AD94 samples, however, were observed to fail along the bond line itself.

3.1.5. Dielectric properties

The data at 2.45 GHz for the real part, ε', and imaginary part, ε'', of the complex permittivity are shown in Fig. 15. Included in the figures are the estimated values which were calculated for the glassy grain-boundary phase present in the lower-purity alumina ceramics using Equation 1. It can be observed that the glass phase properties increase much more rapidly than those of the alumina. The a.c. conductivities were also calculated from the dielectric loss data using Equation 2 and are given in Fig. 16 for both the glassy phase and the AD99.8 alumina. The glass can be seen to be a much better conductor than the alumina and this is believed to account for the ability to heat the lower-purity alumina grades using microwaves. From the Arrhenius plot, an experimental activation energy for the glass conductivity was estimated to be 8.4×10^{-20} J whilst that for the AD99.8 alumina was much lower at 3.03×10^{-20} J.

TABLE V Average four-point flexural strengths of untreated and microwave-joined alumina samples

Material	Strength (MPa)	
	Base material	Joined at 1600 °C and 1 MPa in 10 min
AD85–AD85	264 $\pm$ 53	312 $\pm$ 31
AD94–AD94	282 $\pm$ 68	144 $\pm$ 61

3.2. Diffusion bonding

3.2.1. Scanning electron microscopy observation

Attempts at bonding the AD85 grade ceramic at temperatures below 1400 °C were unsuccessful regardless of pressure or time used. When the AD85 was diffusion bonded for 15 min at 1400 °C and 0.45 MPa, the resultant bond was also clearly evident owing to the lack of contact across the width of the sample. However, when the applied axial pressure was increased to 0.90 MPa, a bond was produced which was undetectable except for a deliberate slight misalignment at the edges. In this respect, the results were very similar to those obtained using microwave bonding. The simultaneous increase in joining temperature to 1600 °C, the axial pressure to 2.7 MPa and the time to 60 min resulted in a bond line which displayed elongated

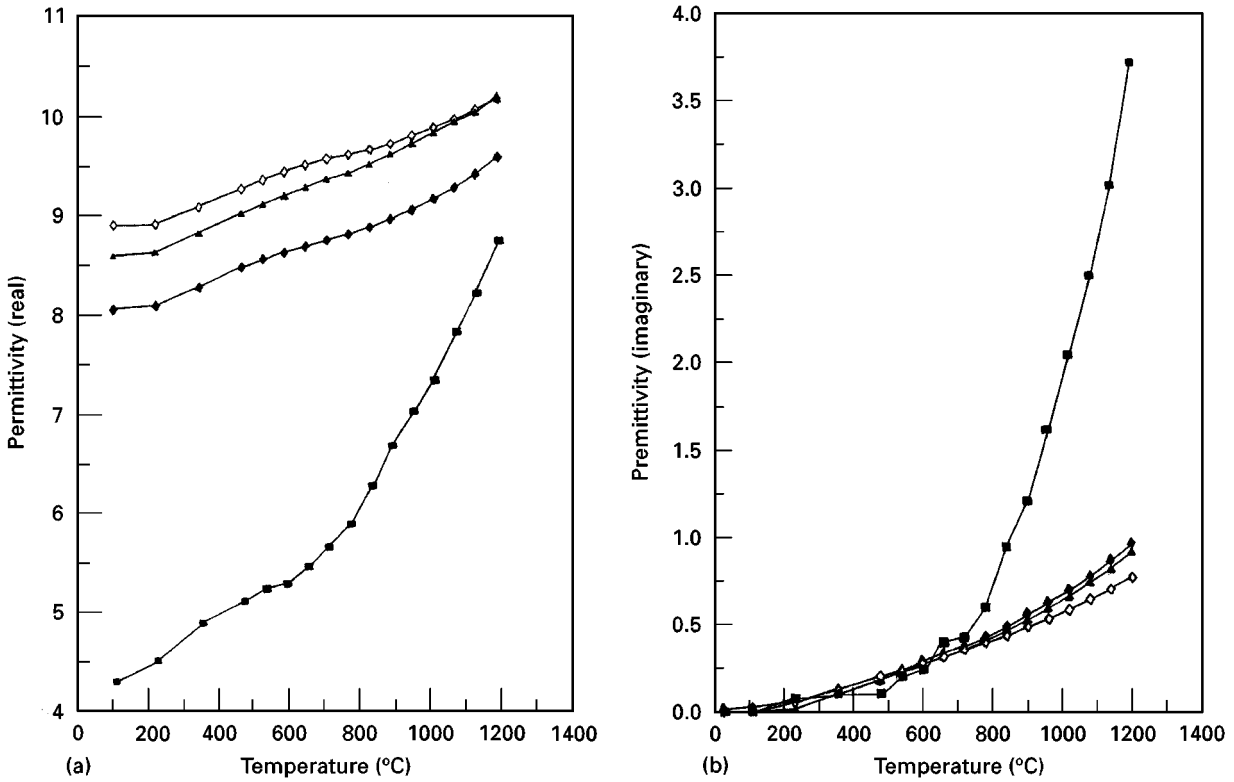

Figure 15 2.45 GHz dielectric properties as a function of temperature: (a) real permittivity, ε'; (b) imaginary permittivity, ε''. (◆), AD85; (▲), AD94; (◇), AD99.8; (■), glass. Values for the grain boundary phase were estimated using Equation 1.

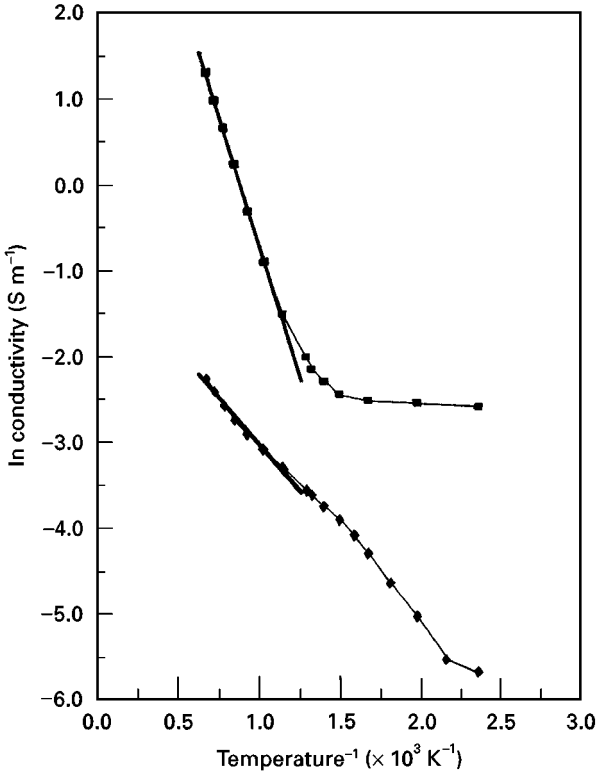

Figure 16 Estimated a.c. conductivities of the glassy grain-boundary phase and AD99.8 as functions of temperature. (–■–), glass; (∿∿∿), glass line fit; (—◆—), AD99.8; (——), AD99.8 line fit.

porosity across the width of the bond, although the amount decreased towards the centre of the samples. However, sectioning the samples approximately 10 mm away from and parallel to the bond revealed extensive cracks running around the sample.

Attempts at joining the AD94 and AD99.8 samples at 1400 °C were unsuccessful regardless of the pressure or time used. An attempt to achieve joining by repeating the 1600 °C, 2.7 MPa, 60 min experiment performed with the AD85 grade for the AD94 grade was also unsuccessful. The bond was clearly visible because of discontinuous contact across the width of the sample, although localized regions of good contact between the grains from opposing surfaces were observed.

3.2.2. Deformation effects

AD85–AD85 samples which were joined using a constant applied axial pressure of 0.90 MPa for a period of 15 min at temperatures of 1200, 1300 and 1400 °C indicated an increase in area strain with temperature from +3.9% to a maximum of +10.9%. All the samples appeared to deform uniformly in a radial direction, causing a slight barrelling effect which spanned about 10 mm on either side of the bond.

3.2.3. Microhardness measurement

The results obtained for the diffusion-bonded alumina samples were very similar to those obtained with microwave bonding. That is, a wide degree of scatter was observed with no statistical variation from the values obtained on the untreated material.

4. Discussion

4.1. Microwave bonding

In agreement with previous reports [1, 2], the lower-purity AD85 and AD94 grades of alumina have been successfully microwave bonded using joining times as short as 10 min and just 150–250 W of power at 2.45 GHz. The direct joining of the AD99.8, alumina was unsuccessful owing to the inability to attain the necessary temperatures, the maximum temperature recorded being 1395 °C.

4.1.1. Scanning electron microscopy observations

The SEM observations made, which are summarized in Table III, indicate that an increase in the applied axial pressure and/or in the bonding temperature improved the contact between the butting surfaces. Under the right conditions it was possible to produce a fully homogeneous microstructure with both the AD85 and the AD94 ceramics, although AD94 required more demanding conditions than AD85. A visual inspection of the AD85 and AD94 bonds indicated that the samples were slightly deformed by the joining process. The region of deformation was, however, restricted to the localized hot zone associated with this technique, which was 10 mm in length and centred on the bond line. Examination of the corresponding deformation measurements indicated that an increase in the level of applied axial pressure and bonding temperature resulted in greater strain, with the temperature appearing to be the most influential for the conditions considered. These results suggest that the applied axial pressure assists in the bonding process by bringing the butting surfaces into contact at their asperities and, with the use of high bonding temperatures, allowed a certain degree of deformation within the hot zone to improve the contact between the butting faces.

Etching of the bond line removed the glassy grain-boundary phase to reveal the location of the grains along the bond. For the AD85 samples joined at 1500 °C and 0.25 MPa, the join was outlined by the rigid positioning of the grains at the butting surfaces as shown in Fig. 7. Increasing the applied axial pressure to 0.5 MPa produced regions where the bond line could not be seen between the opposing grains (Fig. 8). This result suggests that atomic diffusion across the alumina grain boundaries in contact at the join may have occurred. Therefore, the possibility is raised that, if the AD99.8 had been raised to a sufficiently high temperature, then adherence in this manner may have been possible. For the AD85 samples joined at 1600 °C, the grains from opposing faces when brought into contact were able to slide over one another. This rearrangement completely hid the location of the bond. Complete continuity across the bond line was confirmed by the elemental distribution maps for the main constituents of aluminium and silicon, as shown in Fig. 9.

The results suggest that the microwave bonding of alumina was a thermally activated process since temperature appeared to have the greatest influence on

the quality of bond compared with variation in applied axial force. Although the time held at the bonding temperature was not investigated here, previous research has shown that above a critical time the quality of the bond remains consistently high, resulting in bond strengths equalling that of the original material [2].

For the AD94 material, conditions of 1500 °C and 1 MPa resulted in contact between the butting surfaces which appeared to be continuous in SE imaging mode. However, examination using BSE imaging revealed a clear line of glass which filled the bond region with few points of contact between the alumina grains from the opposing faces. An increase in temperature to 1600 °C was required before sufficient grain movement occurred to allow the bond location to remain undetectable even under BSE imaging (Fig. 10).

The presence of the glassy phase therefore appears to have two actions: first, it provides an adhesive medium to hold the butting faces together under intermediate conditions of temperature and pressure and, secondly, under more severe processing conditions, it will allow the alumina grains to rearrange at the join boundary. Walls and Ueki [18] suggested that this rearrangement may well aid in strengthening the join by increasing the diffuse nature of the bond interface. The proposed mechanism is similar to that given by Fukushima *et al.* [1, 2].

The temperature at which the glassy grain-boundary phase begins to soften is dependent on its composition; this in turn is largely dependent on the level of impurities and sintering aids present in the alumina. An analysis of the composition of the glassy grain-boundary phases present in the AD85 and AD94 grades of ceramic [19] suggested a melting temperature in the region of 1700 °C. Softening will have occurred below this temperature and the observed reduction in applied pressure which was noted at 1300–1400 °C indicated where it began to take effect. The softening of the glass allowed greater movement of the alumina grains and explains the improved quality of the bonds produced at higher temperatures. SEM examination of the joins showed no evidence of the glassy grain-boundary phase melting during the microwave heating process and hence, contrary to the ideas of Fukushima *et al.* [2], the bonding process is believed to have relied on the softening and not on the melting of the glassy grain boundary phase. The difference in bonding conditions required for the AD94 material compared with AD85 is believed to be attributable to two factors: first, the lower level of glass present in the higher-purity ceramic but also, secondly, the larger average grain size present. The larger grains are believed to have restricted the ability for grain rearrangement across the bond line and hence reduced the level of bulk deformation occurring. It would have been interesting to have used three grades of alumina ceramic in which the grains sizes were all essentially similar.

One anomaly which should be noted is the variation in microwave heating pattern between the AD85 and AD94 materials. For the AD85 combinations, the edges of the bond region appear to have been slightly cooler than the centre; a 3–5 μm gap was often evident between the butting faces at the edge which extended about 200 μm into the sample. This is consistent with the development of an inverse temperature profile [20]. However, for the AD94 material least contact was observed at the centre of the sample, which would imply that an inverse temperature profile was not established. No explanation for this behaviour can be offered at the present time.

For the AD85–AD99.8 combination, a 5–10 μm glass interlayer at the bond line was a distinct characteristic. The amount of glass present at the join was comparable with that which filled the grain boundaries of the AD85 bulk material. Although there were regions where the alumina grains from the AD85 protruded through the interlayer to make contact with the AD99.8 surface, grain rearrangement in the bond region was negligible. The AD99.8 had the finest grain size of the three grades; however, the almost complete absence of a glassy grain-boundary phase prevented significant movement occurring and no penetration of the AD99.8 by glass from the AD85 was observed. Line profiles for the major constituent elements, aluminium and silicon, also indicated a sharp change in concentration at the AD85–glass–AD99.8 interfaces (Fig. 13). This indicates that atomic diffusion between the ceramic grains and glassy grain-boundary phase was not significant. The electron probe microanalysis line profiles reported by Fukushima *et al.* [2] on the indirect bonding of 99% pure alumina using a 92% pure alumina interlayer also suggested that the microwave bonding of alumina was not conducted by interdiffusion between the glass and ceramic.

The microstructure, grain size and distribution of the three grades of alumina appeared to be unaffected by the microwave heating process. According to Fukushima *et al.* [2], the rapid heating rates associated with microwave heating when compared with conventional processing ensures that the microstructure remains unchanged until temperatures in excess of 1850 °C.

4.1.2. Mechanical properties

The microhardness measurements were performed because previous researchers [2, 3] had observed an increase in hardness across the bond region when compared with the bulk material. A 4 GPa increase in hardness at the join for a 92% pure alumina [2] was attributed to internal distortions within the localized hot zone. However, the results obtained in the current work showed no such trend.

The results of the flexural strength measurements were summarized in Table V. All the AD85 samples fractured away from the bond line and strengths equal to or higher than that of the base material were measured. However, all the AD94 samples fractured along the bond line itself, implying that the SEM observations had not revealed weaknesses present in the bond characteristics. Clearly the conditions of 1600 °C and 1 MPa were not adequate for this grade of alumina and a higher temperature and/or applied axial

pressure are deemed necessary to achieve joins as good as the base material.

4.1.3. Dielectric properties

The dielectric property data for the three grades of alumina (Fig. 15) indicated that the presence of the glassy grain-boundary phase decreases the real part, ε', and increases the imaginary part, ε'', of the permittivity as expected. According to Ho [21], the temperature dependence of ε' is intrinsic to the crystalline lattice properties of the material, suggesting that volumetric expansion accounts for the increase in polarization with increasing temperature. Other physical properties, such as the presence of impurities of a few per cent and microstructure, have only a minor influence on the magnitude and general character of the polarization. However, dielectric losses are far more dependent upon the presence of impurities [21] as is illustrated by the very high calculated value for loss of the glassy grain-boundary phase on its own. It can be seen that above about 700 °C it is the major contributor to the loss of the ceramics and its absence accounts for the inability to heat AD99.8 to a sufficiently high temperature for bonding.

The conductivities from the glassy grain-boundary phase and the AD99.8 alumina are shown in Fig. 16. The observed sharp increase in conductivity and associated high activation energy of 8.43×10^{-20} J for the glassy phase are believed to be a consequence of the softening of this phase. The results of Ho and Morgan [22] support this view.

4.2. Diffusion bonding

AD85 samples could be diffusion bonded to each other under very similar conditions to those required using 2.45 GHz microwave energy. The joins produced at 1400 °C by the two techniques were very similar in terms of both the lack of contact at low axial pressures and the observed grain rearrangement across the join when a pressure of approximately 1 MPa was used. In both cases, the continuity across the join in the latter case was attributed to the glassy grain-boundary phase filling the bond region.

As for the microwave bonding, the use of higher temperatures or pressures increased the area strain deformation during diffusion bonding. However, the deformation zone associated with diffusion bonding spanned a length of 20 mm, i.e., 10 mm on either side of the bond line, which compares unfavourably with the deformation zone of 10 mm for the microwave-bonded material. In addition, the diffusion-bonded samples exhibited a higher area strain. For example, at 1400 °C and 0.9 MPa, AD85 had an area strain of 10.9%, whilst the equivalent microwave-bonded sample (1400 °C and 1 MPa) had an area strain of just 5.6%. Although the time at temperature was very similar for the two bonding techniques, 15 min for diffusion bonding and 10 min for microwave bonding, the total bonding operation, from cold to cold, was very much longer for the diffusion-bonded samples. The reduced time spent close to the bonding temperature and under the applied axial force probably accounts for the lower degree of deformation experienced by the microwave-bonded samples.

Although no strength measurements were performed on the diffusion-bonded samples, the microhardness results were almost identical for the two techniques.

In summary, the results have indicated a definite similarity between the microwave- and diffusion-bonding processes for the joining of alumina ceramics. The observed elongated porosity at the bond line, known to be a distinct characteristic of diffusion bonding, was also found in the microwave heating experiments. A close resemblance was seen between the joining mechanisms present for both techniques and the sintering mechanisms associated with hot pressing. In the AD85 and AD94 ceramics, viscous flow of the glassy grain-boundary phase appeared to be predominant. In regions where direct contact was made between alumina grains in the opposing butting surfaces and in the highest-purity AD99.8 grade ceramic, then there were glimpses of possible evidence for direct atomic diffusion. The one major variation was the processing times required to achieve effectively identical joins. For the diffusion-bonding process a minimum of 2 h was required to achieve a quality join at 1400 °C, whilst an almost identical join could be achieved at the same temperature using microwave energy in just 30 min.

Previous comparisons of the speed with which microwave-bonding [3] and diffusion-bonding processes [23] were performed suggested the possibility that the electromagnetic field contributes a non-thermal mechanism to the process. Janney *et al.* [24] considered the possible lowering of the associated activation energies to enhance diffusion rates and to promote rapid sintering at lower temperatures. Although "the microwave effect" is now a much more established concept and some potentially plausible theories are being put forward [25], no evidence for such an effect was found in this work.

5. Conclusions

The lower the purity of the alumina, the more successful is the microwave-bonding process. This is attributed to two roles being played by the glassy grain-boundary phase present in the lower-purity aluminas.

First, a major function of the glassy phase was to increase the dielectric loss of the host ceramic. The very-high-purity AD99.8 grade did not have much grain-boundary phase and hence was insufficiently lossy to couple with the microwave energy and so could not be heated. The microwave heating mechanism in these materials is thus primarily associated with the losses provided by the glassy grain-boundary phase.

Secondly, the bonding mechanism was based on viscous flow of the glassy grain-boundary phase. By softening, the glassy phase allowed the alumina grains to move under the imposed load. Provided that sufficient migration across the bond line of both glassy phase and grains occurred, then a fully homogeneous

microstructure could be obtained in which no obvious glassy line existed at the boundary, making it indistinguishable from the bulk material. This mechanism was valid for both microwave bonding and conventional diffusion bonding.

Despite the similarity in bonding mechanism, microwave bonding can be a factor of at least 4 faster than diffusion bonding and results in significantly less deformation of the samples. The low-purity alumina ceramics could be microwave bonded, without the use of interlayers, with bonding times of about 10 min and total processing times of only about 30–40 min. The principal reason for this is the efficiency of energy transfer in the microwave case.

For the 85% pure alumina the mechanical strength of the join was as high as or higher than that of the parent material with the bonded samples never breaking at the bond line during four-point bend tests. The conditions were not sufficiently optimized for the 94% pure alumina and the joins always failed at the bond line.

Some evidence was also found for the bonding of individual grains where they came into direct contact across the bond line. This implies that direct joining of high-purity aluminas without a substantial glassy grain-boundary phase may be possible if sufficient contact can be ensured between the mating faces and sufficiently high temperatures and pressures are used. A means of increasing the losses of the system to allow sufficient energy to be deposited in the ceramic would be required. One solution might be to use pre-heating of the samples.

Acknowledgements

The authors would like to acknowledge the financial contribution made to this project by TWI and the Engineering and Physical Science Research Council, both in the UK.

References

1. H. FUKUSHIMA, T. YAMANAKA and M. MATSUI, in "Microwave processing of materials", Materials Research Society Symposium Proceedings, Vol. 124, edited by W. H. Sutton, M. H. Brooks and I. J. Chabinsky (Materials Research Society, Pittsburgh, PA, 1988) pp. 267–72.
2. *Idem*., *J. Mater. Res.* **5** (1990) 397.
3. D. PALAITH, R. SILBERGLITT, C. C. M. WU, R. KLEINER and E. L. LIBELO, in "Microwave processing of materials", Materials Research Society Symposium Proceedings, Vol. 124, edited by W. H. Sutton, M. H. Brooks and I. J. Chabinsky (Materials Research Society, Pittsburgh, PA, 1988) pp. 255–66.
4. T. T. MEEK and R. D. BLAKE, US Patent 4 529 857 (1985).
5. *Idem*., *J. Mater. Sci. Lett*. **5** (1986) 270.
6. S. AL-ASSAFI, I. AHMAD, Z. FATHI and D. E. CLARK, *Ceram. Trans.* **21** (1991) 515.
7. S. AL-ASSAFI and D. E. CLARK, in "Microwave processing of materials III", Materials Research Society Symposium Proceedings, Vol. 269, edited by R. L. Beatty, W. H. Sutton and M. F. Iskander (Materials Research Society, Pittsburgh, PA, 1992) pp. 355–40.
8. S. AL-ASSAFI and D. E. CLARK, *Ceram. Engng Sci. Proc.* **2** (1992) 1073.
9. P. S. APTÉ, R. M. KIMER and M. C. L. PATTERSON, Report prepared for the Ontario Ministry of Energy, Project 600049, Alcan International Ltd, Kingston Research and Development Centre, Kingston, Ontario, Canada (1988).
10. X. D. XU, V. V. VARADAN and V. K. VARADAN, in microwaves: Theory and Application in Materials Processing, Ceramic Trans. Vol. 21 (D. E. Clark. F. O. Gac and W. H. Sutton, ACers, Westerville, 1991) p. 497.
11. I. AHMAD and W. M. BLACK, *Ceram. Engng Sci. Proc.* **1** (1992) 520.
12. I. AHMAD, R. SILBERGLITT, W. M. BLACK, H. S. SA'ADALDIN and J. D. KATZ, in "Microwave processing of materials III", Materials Research Society Symposium Proceedings, Vol. 269, edited by R. L. Beatty, W. H. Sutton and M. F. Iskander (Materials Research Society, Pittsburgh, PA, 1992) pp. 271–76.
13. T. Y. YIIN, V. V. VARADAN, V. K. VARADAN and J. C. CONWAY, in microwaves: Theory and Application in Materials Processing, Ceramic Trans. Vol. 21 (D. E. Clark. F. O. Gac and W. H. Sutton, ACers, Westerville, 1991) p. 507.
14. T. SATO, T. SUGIURA and K. SHIMAKAGE, *J. Ceram. Soc. Jpn* **101** (1993) 422.
15. R. SILBERGLITT, D. PALAITH, H. S. SA'ADALDIN, W. M. BLACK, J. D. KATZ and R. D. BLAKE, *ibid.* **101** (1993) 487.
16. M. ARAI, J. G. P. BINNER, G. E. CARR and T. E. CROSS, in microwaves: Theory and Application in Materials Processing, Ceramic Trans. Vol. 21 (D. E. Clark. F. O. Gac and W. H. Sutton, ACers, Westerville, 1991) p. 483.
17. S. O. NELSON and T-S. YOU, *J. Phys. D* **23** (1990) 346.
18. P. A. WALLS and M. UEKI, *J. Amer. Ceram. Soc.* **75** (1992) 2491.
19. P. A. DAVIS, PhD thesis, The University of Nottingham, Nottingham (1995).
20. J. G. P. BINNER and T. E. CROSS, *J. Hard Mater.* **4** (1993) 177.
21. W. W. HO, in "Microwave processing of materials", Materials Research Society, Symposium Proceedings, Vol. 124, edited by W. H. Sutton, M. H. Brooks and I. J. Chabinsky (Materials Research Society, Pittsburgh, PA, 1988) pp. 137–48.
22. W. W. HO and P. E. D. MORGAN, *J. Amer. Ceram. Soc.* **70** (1987) C209.
23. C. SCOTT and V. B. TRAN, *Ceram. Bull.* **64** (1985) 1129.
24. M. A. JANNEY, C. L. CALHOUN and H. D. KIMREY, *J. Amer. Ceram. Soc.* **75** (1992) 341.
25. K. I. RYBOKOV, V. E. SEMENOV, S. A. FREEMAN, J. H. BOOSKE and R. F. COOPER, in Microwave Processing of Materials V, Materials Research Society, Symposium Proceedings, Vol. 430 (M. F. Iskander, J. O. Kiggens Jr, J-C. Boloney (eds.), Materials Research Society, Pittsburgh, P.A., 1996) p. 459

Received 19 August 1997
and accepted 3 March 1998